Journal of Applied Electrochemistry **34**: 1071–1080, 2004.

Electrochemical behaviour of Al, Al–In and Al–Ga–In alloys in chloride solutions containing zinc ions

S. ZEIN EL ABEDIN[1] and F. ENDRES[2]*
[1]*Electrochemistry and Corrosion Laboratory, National Research Centre, Dokki, Cairo, Egypt*
[2]*Institute of Metallurgy, Robert-Koch-Strasse 42, 38678 Clausthal-Zellerfeld, Germany*
*(*author for correspondence, fax: +49-(0)5323722460, e-mail: frank.endres@tu-clausthal.de)*

Received 9 September 2003; accepted in revised form 25 May 2004

Key words: activation, aluminium, aluminium alloys, corrosion, zinc ions

Abstract

The electrochemical behaviour of Al, Al–In and Al–Ga–In alloys in 0.6 M NaCl solutions with and without Zn^{2+} was investigated. The study was performed by means of open circuit potential, potentiodynamic polarization, potentiostatic current-time and electrochemical impedance spectroscopy measurements as well as by SEM-EDAX examination. It was found that the Al–In alloy exhibits the highest negative open circuit potential in 0.6 M NaCl and the corrosion resistance of the tested electrodes decreases in the following order: Al > Al–Ga–In > Al–In. The greater activity of the Al–In alloy was interpreted on the basis of the autocatalytic attack by indium. The potentiostatic current–time measurements in Zn^{2+} containing electrolyte at potentials above the pitting potential revealed that Zn^{2+} has an insignificant influence on the Al electrode, while it enhances the corrosion of the Al–Ga–In alloy and improves the attack morphology of the Al–In alloy. Furthermore, the impedance spectra recorded under open circuit conditions showed a decrease in the polarization resistance of Al–In and Al–Ga–In alloys in presence of Zn^{2+} indicating the activating effect of Zn^{2+} ions.

1. Introduction

Aluminium and aluminium alloys are widely used and have great economic importance in view of their low cost, light weight and good corrosion resistance. Due to weight and cost advantages aluminium is the most commonly used sacrificial material for cathodic protection of steel in seawater.

The most important factor in the use of aluminium in aqueous electrolytes is that complex oxide films are formed irreversibly leading to passivation. Pure aluminium supports a passive film on the surface with an open circuit potential of about −0.800 V vs SCE in seawater [1] which makes it useless as a sacrificial anode in cathodic protection of steel in seawater. This film is relatively stable in aqueous solutions over a pH range of 4 to 8.5 [2]. The passivity of aluminium can be overcome by adding suitable alloying elements such as Sn [3–8], In [9–13], Zn [14, 15] and Ga [16–18]. Activation of aluminium can also be achieved by adding small quantities of suitable metal cations, such as In^{3+}, Ga^{3+}, Hg^{2+}, Sn^{4+} and Sn^{2+}, to the solution [19–27]. It was reported [28] that addition of Ga^{3+} causes activation of aluminium in 0.6 M NaCl solution, but only at a slow rate. Much higher concentrations of Ga^{3+} were required to achieve activation. Breslin et al. [24, 29] stated that the onset of passivity breakdown of aluminium by gallium ions in chloride solutions was less efficient. It was demonstrated [30] that the activation of aluminium by In^{3+} depends on the chloride ion concentration, the surface finish of the samples and the purity of the metal. Addition of In^{3+} [31] produced activation of pure Al, Al–Zn and Al–Zn–Sn alloys in 0.6 M NaCl solution. The existence of Zn either as an alloying element or as a cation in the electrolyte leads to an enhanced activity of aluminium in the presence of In^{3+} ions [31]. Furthermore, at one and the same concentration of In^{3+}, the corrosion rate of pure Al in 0.6 M NaCl increases by increasing the concentration of Zn^{2+}. Breslin et al. [12, 32] suggested that the presence of zinc promotes the nucleation of $ZnAl_2O_4$ spinel which gives rise to increased defects and cracking of the protective layer.

Therefore, as a continuation of our work on the activation of aluminium, it seemed of interest to examine the effect of Zn^{2+} ions on the electrochemical behaviour of Al, Al–In and Al–Ga–In alloys in chloride solutions and to shed further light on the role of zinc on the activation process. The study comprised open circuit potential, potentiodynamic polarization, potentiostatic current-time and electrochemical impedance spectroscopy measurements as well as SEM-EDAX examination.

Table 1. Chemical composition of the alloys (weight %)

Alloy	Fe	Si	Cu	Pb	Mn	Mg	Zn	In	Ga	Al
Al–In	0.095	0.045	0.005	0.001	0.0005	0.0005	0.0005	0.77	–	Rest
Al–Ga–In	0.08	0.03	0.005	0.001	0.0005	0.0005	0.0005	0.21	0.40	Rest

2. Experimental details

Measurements were made on ultra pure Al (99.999%), Al–In and Al–Ga–In alloys, the composition of the alloys is given in Table 1. Al–In and Al–Ga–In alloys were prepared from pure aluminium (99.99%), ultrapure In (99.999%) and Ga (99.999%). Aluminium and the alloying elements were melted in vacuum-sealed quartz tubes in a muffle furnace and were cooled down to the ambient temperature in the furnace. Because of mixing difficulties, the alloys were melted again in a graphite crucible and stirred with a graphite rod. Alloy melts were then poured into a rectangular iron mould and left to cool in air. The prepared alloys were used in the cast state.

Prior to each experiment the working electrodes were successively abraded with metallographic emery paper of increasing fineness up to 800, then degreased with acetone and washed with distilled water and then inserted immediately into the cell. The electrochemical cell was made of Pyrex glass fitted with a large area platinum auxiliary electrode and a saturated calomel reference electrode (SCE) connected through a salt bridge. All solutions were prepared from Analar grade reagents and distilled water.

All electrochemical measurements were performed using a Parstat 2263 potentiostat/galvanostat (Princeton Applied Research) controlled by a PowerCORR corrosion measurement software and a PowerSINE electrochemical impedance spectroscopy software. The impedance spectra were recorded under open circuit conditions in the frequency range between 100 kHz and 100 mHz with an amplitude of 10 mV. The data were fitted and evaluated using a ZsimpWin electrochemical impedance spectroscopy analysis software. The tested electrodes were cathodically polarized at −2000 mV vs SCE for 3 min in the test electrolytes before potentiodynamic polarization and potentiostatic current–time measurements. This is to remove the air-formed oxide layer and to get a reproducible quasi bare aluminium surface. In the potentiodynamic polarization measurements, a scan rate of 1 mV s^{-1} was employed and the potential was scanned from −2.0 V up to the breakdown potential. A scanning electron microscope (CamScan) attached with energy dispersive X-ray analyser (EDAX) was utilized to examine the electrode surface.

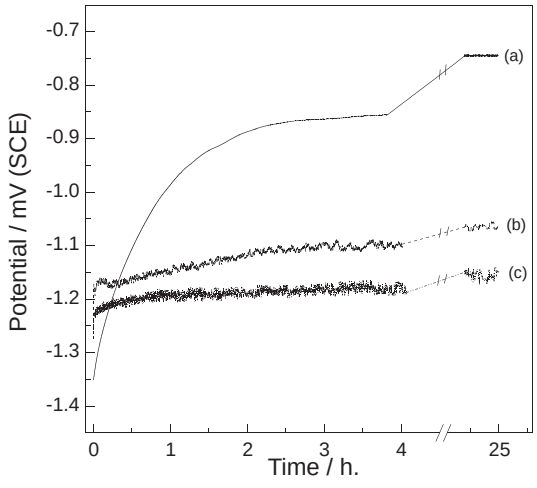

Fig. 1. Variation of the open circuit potential of (a) Al, (b) Al–Ga–In and (c) Al–In electrodes with time in 0.6 M NaCl.

3. Results and discussions

3.1. *Open circuit potential*

The curves of Figure 1 display the open circuit potential of Al, Al–In and Al–Ga–In electrodes in 0.6 M NaCl solutions as a function of time. The potential of the Al electrode moves in the positive direction reaching a quasi-steady state value after about 100 min. This can be attributed to the formation of oxide films at the electrode surface leading to the ennoblement of the electrode potential. The electrode attains a stable steady state potential of −768 mV after 24 h. On the other hand, potential fluctuations, which span a ~20 mV range, are observed with Al–In alloy from the beginning and lasted throughout the experiment, indicating an activation-repassivation process. This can be ascribed to the presence of indium in the alloy, which enhances the adsorption of Cl^- ions at the electrode surface leading to the observed activity. Al–Ga–In alloy exhibits an approximately similar behaviour as that of Al–In alloy but the potential fluctuations are of lower magnitude, about 10 mV, and the potential is less negative than the potential of Al–In alloy. This can be attributed to the presence of Ga and not to the lower percentage of In content in the alloy (0.21% In) compared to Al–In alloy (0.77% In). It was reported [11] that the electrochemical behaviour of Al–0.09% In and Al–5% In is practically the same. Hence the difference in the In content in the alloys plays no role on the electrochemical behaviour of the tested alloys. Therefore, it can be concluded that Ga improves, to some extent, the attack morphology of the alloy and exerts some sort of passivity to the alloy as evidenced by the reducing magnitude of potential fluctuations and the lower negative open circuit potential compared to Al–In alloy. It was, also, found [33]

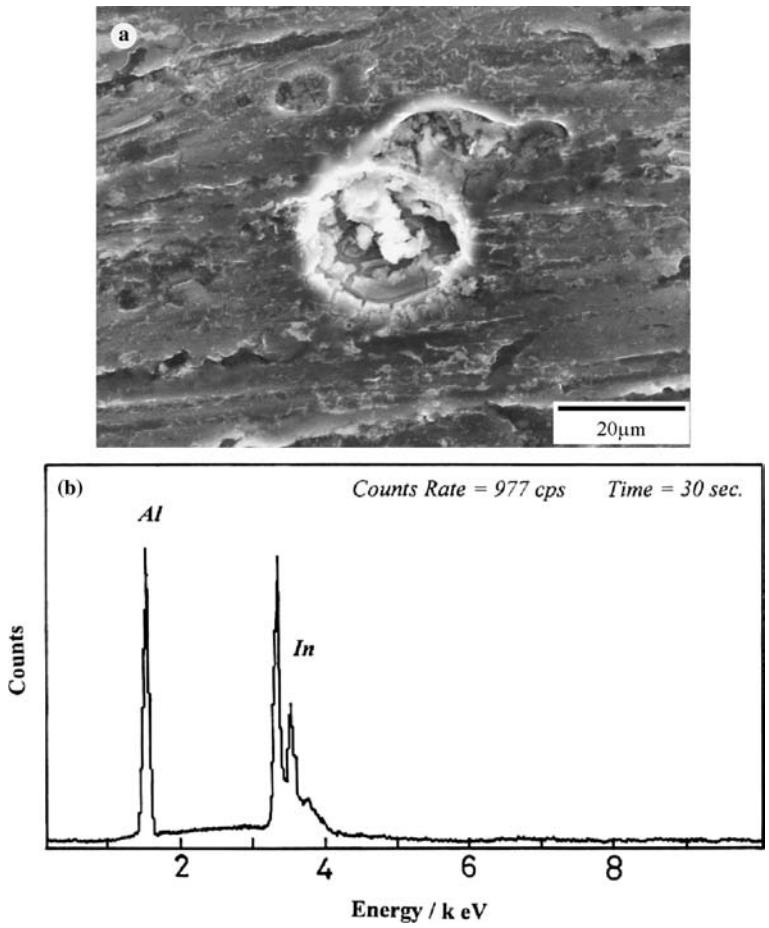

Fig. 2. (a) SEM micrograph of Al–In alloy obtained after ocp measurement in 0.6 M NaCl for 24 h; (b) EDAX analysis inside the pit shown in the micrograph.

that the presence of Ga improves the corrosion resistance of Al–Ga–In alloy in alkaline media.

Surface examination of the Al–In electrode by SEM, Figure 2(a), after open circuit potential measurements in 0.6 M NaCl for 24 h showed localized attack with typical pits in the early stages of development. The pits contain indium as detected by the accompanying EDAX profile, Figure 2(b), indicating an autocatalytic attack by indium. An autocatalytic mechanism has been suggested by Reboul et al. [14] to account for the activity of mercury and indium-activated aluminium in which dissolution of the anode introduces both aluminium and activator ions into the solution and then the activator species deposits, subsequently, giving rise to further dissolution of the anode. Accordingly, the initial dissolution of the Al–In electrode leads to an increase in the concentration of In^{3+} ions in the electrolyte, then the redeposition of In at the active sites occurs. This leads to the adsorption of Cl^- at high negative potential owing to the greater affinity of In for Cl^- [34]. Once a sufficient amount of indium metal has been redeposited on the defect centres of the oxide film, the surface Cl^- ion concentration increases and approaches that observed at the pitting potential. Then Cl^- penetrates the surface layers leading to the observed pitting attack at higher negative potential compared with that of pure aluminium.

3.2. *Potentiodynamic polarization*

The potentiodynamic polarization curves of pure Al, Al–In and Al–Ga–In alloys in 0.6 M NaCl solution are shown in Figure 3. The polarization curve of Al is characterized by a broad passive region extending for about 820 mV from −1580 to −760 mV vs SCE over which the passive current is about 6 μA cm^{-2}. This passive behaviour has been documented by previous workers [30, 35, 36] and is attributed to the formation of protective oxide films on the aluminium surface. At the end of the passive region the current increases abruptly as a consequence of the pitting initiation process and hence the passivity breakdown.

Al–In alloy exhibits different behaviour from that of pure aluminium, since the polarization curve shows an active behaviour without any passivity. The pitting potential takes a value close to the corrosion potential signifying the greater activity of the alloy compared to pure aluminium. This is attributable to the presence of In as an alloying element, giving rise to increased Cl^- adsorption at higher negative potential which, in turn, leads to the observed activity.

The polarization curve of Al–Ga–In alloy is characterized by a major anodic peak followed by a gradual active to passive transition evidenced by more than one

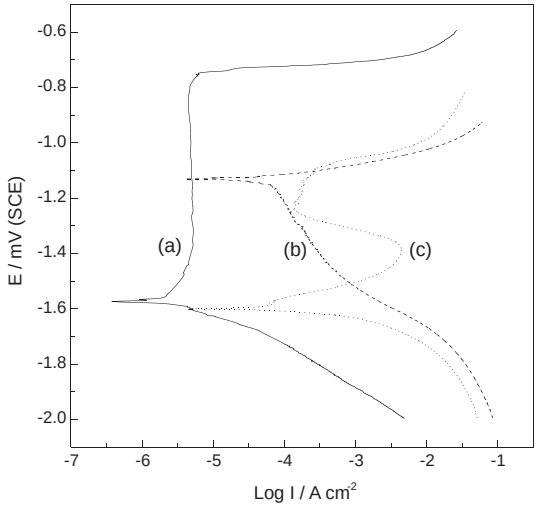

Fig. 3. Potentiodynamic polarization curves of (a) Al, (b) Al–In and (c) Al–Ga–In electrodes in 0.6 M NaCl.

order of magnitude decrease in the current. This peak has also been observed by Tuck et al. [16] and represents the oxidation of Ga. Beyond the peak a small passive region of about 200 mV is observed followed by a rapid increase in the anodic current indicating the start of pitting attack.

The effect of adding different concentrations of Zn^{2+} on the polarization behaviour of Al, Al–In and Al–Ga–In alloys in 0.6 M NaCl solutions was investigated, Figure 4. As shown in Figure 4(a), the cathodic branch of the polarization curves of the Al electrode is strongly affected by adding Zn^{2+} to the electrolyte and moves to higher current densities with increasing concentration of Zn^{2+}. This can be ascribed to the deposition of Zn which is evidenced by the reduction steps observed on the cathodic arm of the polarization curves. The corrosion potential moves towards the positive direction with increasing concentration of Zn^{2+} and approaches a value of −1040 mV, which is close to the corrosion potential of zinc metal in chloride solutions. The corrosion potential of zinc in 0.5 M NaCl solution of pH 5 was recorded to be about −1070 mV vs SCE [37]. This indicates that the electrode was covered by a deposited layer of zinc. The peak observed on the anodic arm of the polarization curves can be explained in terms of the oxidation of elemental zinc to $Zn(OH)_2$ [38]. The pitting potential of the Al electrode shows a slight shift in the negative direction with increase in Zn^{2+} content.

The polarization curves of Al–In alloy in 0.6 M NaCl free and containing different concentrations of Zn^{2+} are displayed in Figure 4(b). As in the case of pure Al, a reduction step, due to the deposition of Zn, was observed on the cathodic branch of the polarization curves and was found to be more pronounced with increasing concentration of Zn^{2+}. Moreover, the corrosion potential takes values close to that of Zn metal. As shown in the polarization curves, addition of Zn^{2+} alters the anodic behaviour of the alloy, where the anodic current increases exponentially with the potential indicating active dissolution of the alloy. However, in the case of Zn^{2+} free electrolyte the anodic current increases abruptly as a result of the pitting attack.

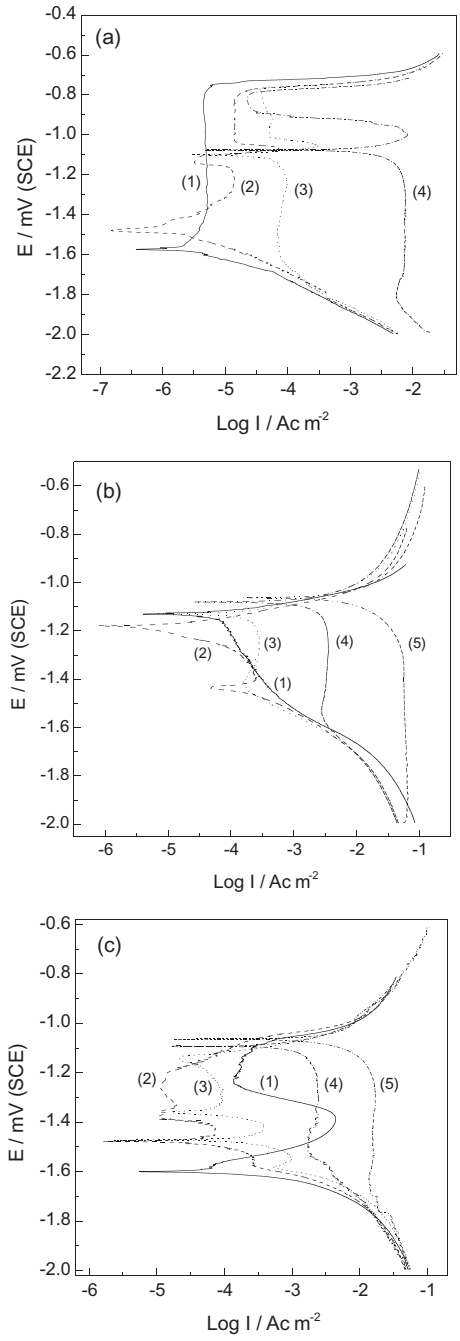

Fig. 4. Potentiodynamic polarization curves of (a) Al, (b) Al–In and (c) Al–Ga–In electrodes in 0.6 M NaCl and different concentrations of Zn^{2+}. Curves (1) without Zn^{2+}, (2) 10^{-2} M Zn^{2+}, (3) 5×10^{-2} M Zn^{2+} and (4) 10^{-1} M Zn^{2+} for Al. Curves (1) without Zn^{2+}, (2) 10^{-4} M Zn^{2+}, (3) 10^{-2} M Zn^{2+}, (4) 5×10^{-2} M Zn^{2+} and (5) 10^{-1} M Zn^{2+} for Al–In and Al–Ga–In alloys.

The surface of the electrode was inspected using SEM-EDAX after polarization measurements in 0.6 M NaCl free, Figure 5, and containing 0.01 M Zn^{2+}, Figure 6, with the objective of demonstration the effect of Zn^{2+} on the attack morphology of Al–In alloy. As seen in Figure 5(a), the surface exhibits pitting attack and

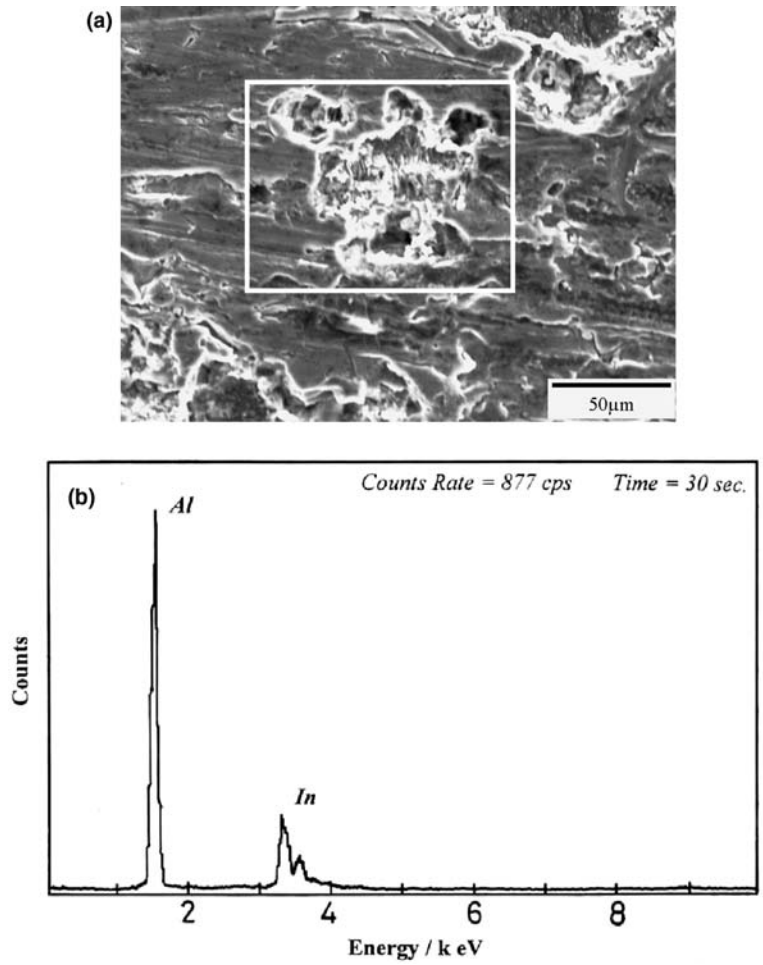

Fig. 5. (a) SEM micrograph of Al–In alloy obtained after potentiodynamic polarization measurement in 0.6 M NaCl; (b) EDAX analysis within the pit shown in the micrograph.

within the pits indium was detected as revealed from the corresponding EDAX spectrum, Figure 5(b). The same attack morphology was recorded for pure Al after potentiostatic polarization at −1050 mV in 0.6 M NaCl containing 5×10^{-3} M In^{3+} [30]. This finding supports the autocatalytic attack mechanism by indium via dissolution and redeposition of In on the active sites. On the other hand, only a few small pits were detected on the surface after polarization in 0.01 Zn^{2+} containing electrolyte, Figure 6(b). The surface is covered by a deposited layer of zinc, as revealed from the EDAX profile of Figure 6(a) and the white spots shown in the SEM micrograph were analysed as indium, Figure 6(c).

The presence of Zn^{2+} enhances the redeposition process of In on the electrode surface where indium deposition is easier on zinc than on aluminium sites [25]. This is indicated by the greater amount of In spots on the electrode surface after polarization measurements in Zn^{2+} containing electrolyte, Figure 6(b). Moreover, as a consequence of Zn deposition, sufficient nucleation of $ZnAl_2O_4$ spinel occurs and causes rupture and defects of the surface layers promoting the active sites for redeposition of In. The formation of $ZnAl_2O_4$ spinel was detected by XPS analysis of Al–Zn alloy in a former study [27]. Therefore, it can be concluded that the surface enrichment by In, as a consequence of zinc deposition, gives rise to the adsorption of Cl^- at more negative potential and ensures an active state of the electrode. Moreover, the presence of Zn^{2+} improves the attack morphology of Al–In alloy which is a prerequisite for a good anode.

Al–Ga–In alloy exhibits similar results as in the case of Al–In alloy with addition of Zn^{2+} to the electrolyte, Figure 4(c). The corrosion potential shifts in the positive direction with increasing concentration of Zn^{2+} as a result of Zn deposition and reaches a value close to that of zinc metal. The anodic current increases regularly with potential indicating active dissolution of the alloy. The oxidation peak of Ga does not appear on the anodic branch of the polarization curves at higher concentrations of Zn^{2+} ($C > 10^{-2}$ M Zn^{2+}). This is attributable to the greater amount of deposited Zn which covers Ga atoms on the surface.

3.3. *Current–time measurements*

The effect of adding different concentrations of Zn^{2+} (10^{-3}–10^{-1} M) on the I/t profile of Al–In alloy polarized

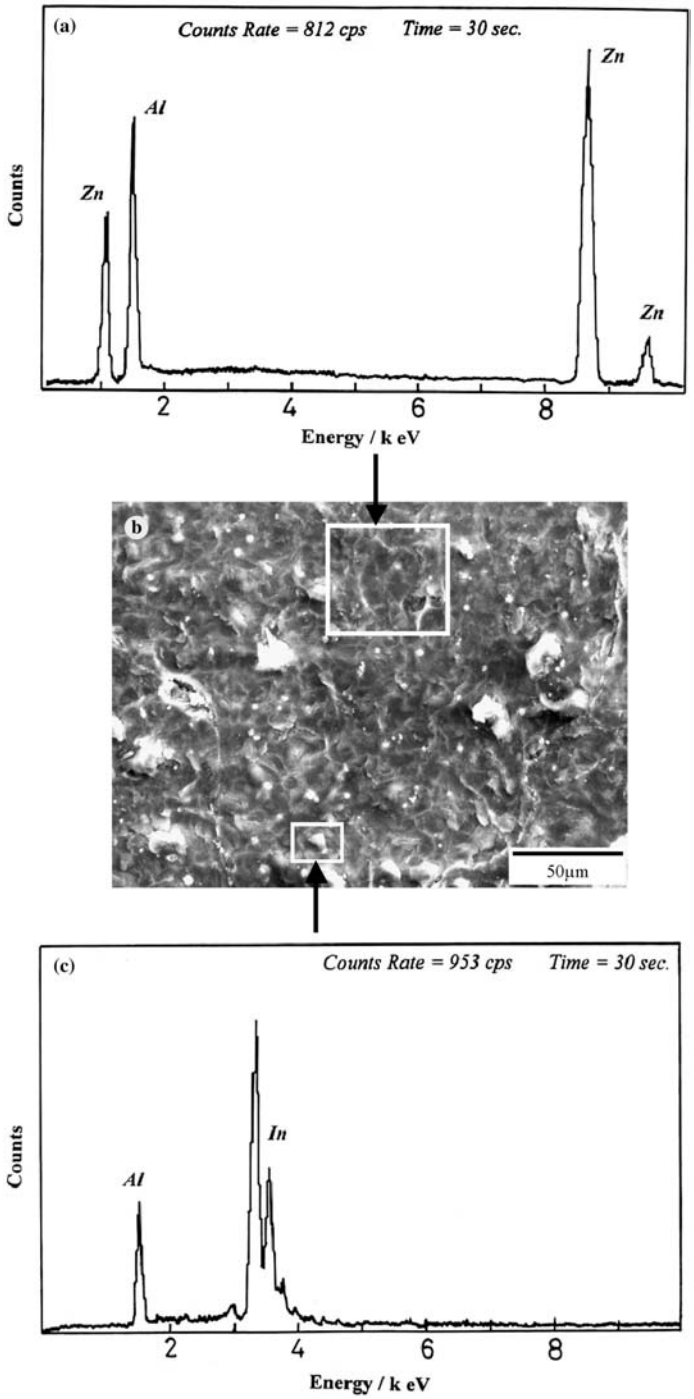

Fig. 6. (a) EDAX analysis for the area shown in the upper part of the SEM micrograph of Figure 6(b); (b) SEM micrograph of Al–In alloy obtained after potentiodynamic polarization measurement in 0.6 M NaCl and 0.01 M Zn^{2+}; (c) EDAX analysis for the particle shown in the lower part of the SEM micrograph of Figure 6(b).

at −1050 mV vs SCE in 0.6 M NaCl is shown in Figure 7(a). The applied potential (−1050 mV) was chosen to be less negative than the pitting potential to show the role of Zn^{2+} on the corrosion process under anodic conditions. In 0.6 M NaCl without Zn^{2+}, the anodic current increases rapidly in the early moments due to double layer charging. Then the anodic current decreases with fluctuation signifying pitting attack. Here, the anodic current represents both the propagation of the first pits and the initiation of new pits and the oscillating nature of the current is due to the repeated birth and death of pits [39]. Approximately the same general features are observed in the absence and presence of Zn^{2+}, but increasingly the anodic current decreases in the early stages. This can be attributed to the deposition of Zn which increases with increasing concentration of Zn^{2+}. The electrochemical deposition of Zn at this potential (−1050 mV) is expected, since the standard equilibrium potential of Zn/Zn^{2+} is about −982 mV vs SCE. After this, the current increases

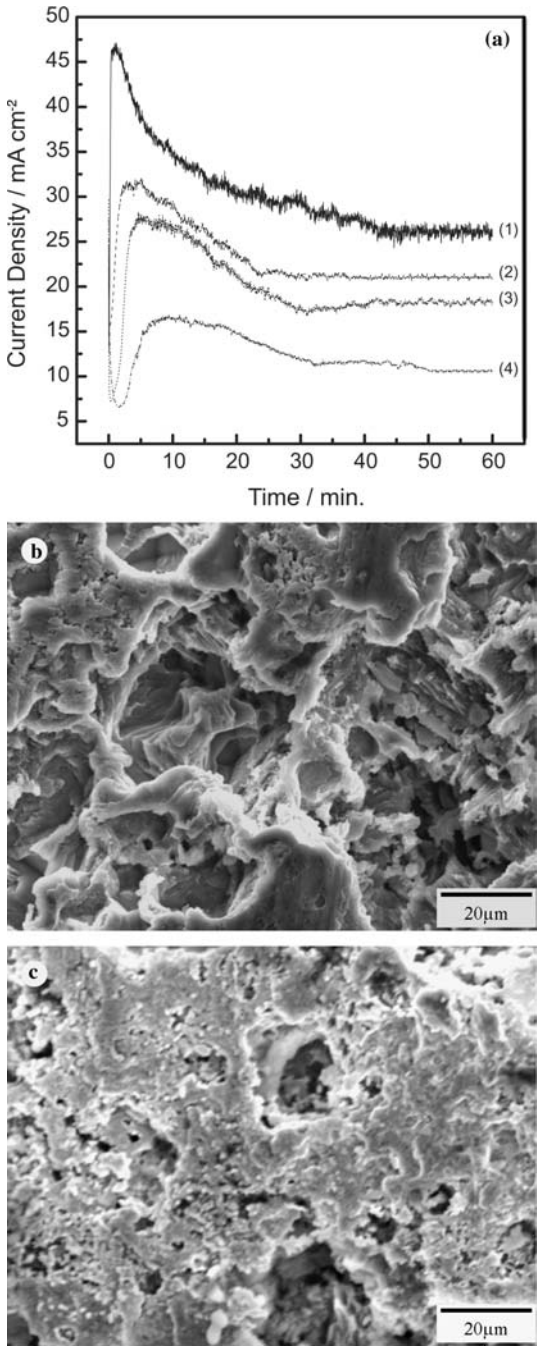

Fig. 7. (a) Current–time curves for Al–In alloy polarized at −1050 mV in 0.6 M NaCl and different concentrations of Zn^{2+}. Curves (1) without Zn^{2+}, (2) 10^{-3} M Zn^{2+}, (3) 10^{-2} M Zn^{2+} and (4) 10^{-1} M Zn^{2+}. SEM micrographs of Al–In alloy obtained after potentiostatic current–time measurement at −1050 for 1 h in (b) 0.6 M NaCl and (c) 0.6 M NaCl + 0.01 M Zn^{2+}.

until reaching a maximum then begins to fluctuate, signifying the initiation of pitting attack. A further decrease is then recorded up to an approximately constant value. This is due to the further deposition of Zn which proceeds until the electrode surface is covered and no further deposition occurs, as shown by the constancy of the current. In general, the anodic current decreases as the concentration of Zn^{2+} increases which indicates the reducing, to some extent, of the aggressiveness of corrosion under such severe conditions. SEM micrographs taken after I/t measurements in 0.6 M NaCl free, Figure 7(b), and containing 0.01 M Zn^{2+}, Figure 7(c), support the above results. As shown in Figure 7(b), the attack appears to be severe and destructive in the absence of Zn^{2+}, while in the presence of 0.01 Zn^{2+}, Figure 7(c), the attack is not as strong as in absence of Zn^{2+}. This can be ascribed to the plating out of zinc on the electrode surface, as detected by EDAX analysis (no spectrum is shown), which suppresses, to some extent, the severe corrosion and improves the attack morphology and hence improves the anode efficiency.

Figure 8(a) shows the current-time profiles for Al–Ga–In alloy polarized at −1000 mV in 0.6 M NaCl with and without different concentrations of Zn^{2+} (10^{-3} – 10^{-1} M). As in case of Al–In alloy the potential of −1000 mV was chosen to be more anodic than the breakdown potential to demonstrate the effect of Zn^{2+} on the corrosion of Al–Ga–In under anodic conditions. As manifested in Figure 8(a), the current increases with increasing Zn^{2+} concentration which indicates the accelerating effect of Zn^{2+} on the corrosion of Al–Ga–In alloy under such anodic conditions. This situation is confirmed by SEM examination of the surface of Al–Ga–In electrode after I/t measurements at −1000 mV in 0.6 M NaCl with and without 0.01 M Zn^{2+}. In the absence of Zn^{2+}, numerous small pits are seen in the SEM micrograph of Figure 8(b). However, in presence of 0.01 M Zn^{2+}, the attack is severe and the pits grow laterally, forming cavities as shown in Figure 8(c). The addition of Zn^{2+} has insignificant influence on the potentiostatic current-time behaviour of Al in 0.6 M NaCl solutions and hence on the activation process (no figures are shown). This can be attributed to the tendency of zinc to dissolve from the surface after deposition, combined with its much lower mobility into the bulk metal. Moreover, aluminium should be protected cathodically at the expense of the deposited zinc and, consequently, dissolution of zinc takes place from the surface.

In the light of the potentiostatic I/t measurements, it can be concluded that under such anodic conditions, additions of Zn^{2+} improves the attack morphology of Al–In alloy, while it accelerates the corrosion of Al–Ga–In alloy and has insignificant influence on pure Al.

3.4. *Electrochemical impedance spectroscopy*

In the present work, the impedance technique was used as a basis for a comparative study to show the corrosion behaviour of the tested electrodes in Cl^- solutions as well as the effect of Zn^{2+} addition. The electrochemical impedance spectroscopy of Al, Al–In and Al–Ga–In alloys was recorded under open circuit conditions in 0.6 M NaCl solutions free of and containing 0.01 M Zn^{2+}. The measurements were performed after immersion of the electrodes in the test electrolytes for 2 h in order to obtain steady state conditions. Figure 9 shows

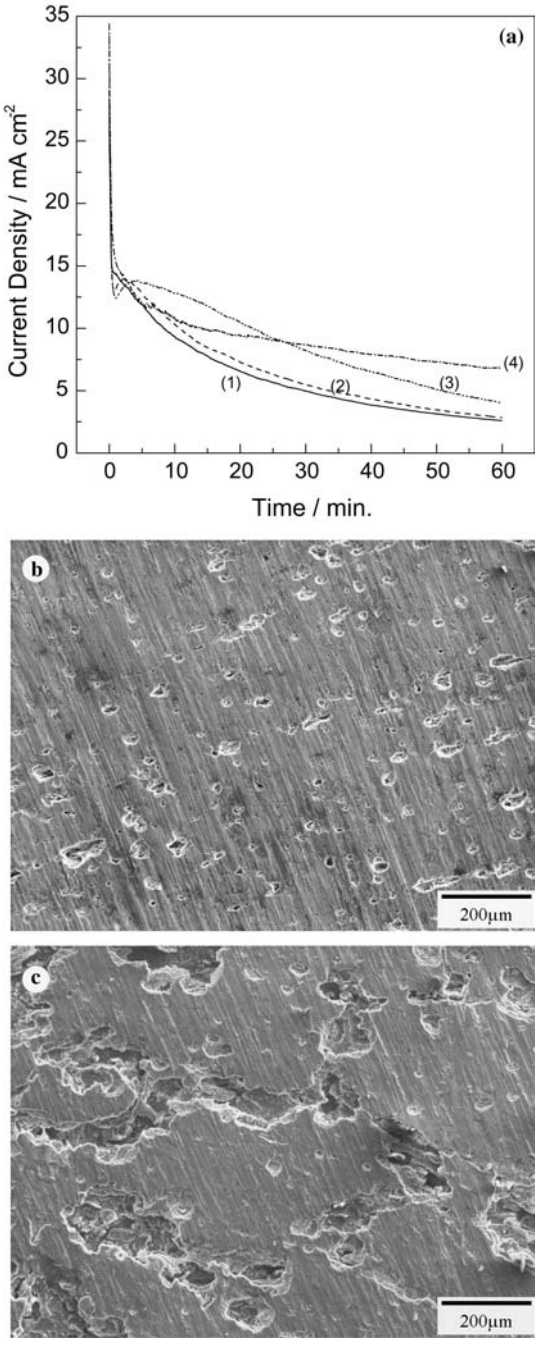

Fig. 8. (a) Current–time curves for Al–Ga–In alloy polarized at −1000 mV in 0.6 M NaCl and different concentrations of Zn^{2+}. Curves (1) without Zn^{2+}, (2) 10^{-3} M Zn^{2+}, (3) 10^{-2} M Zn^{2+} and (4) 10^{-1} M Zn^{2+}. SEM micrographs of Al–Ga–In alloy obtained after potentiostatic current-time measurement at −1000 for 1 h in (b) 0.6 M NaCl and (c) 0.6 M NaCl + 0.01 M Zn^{2+}.

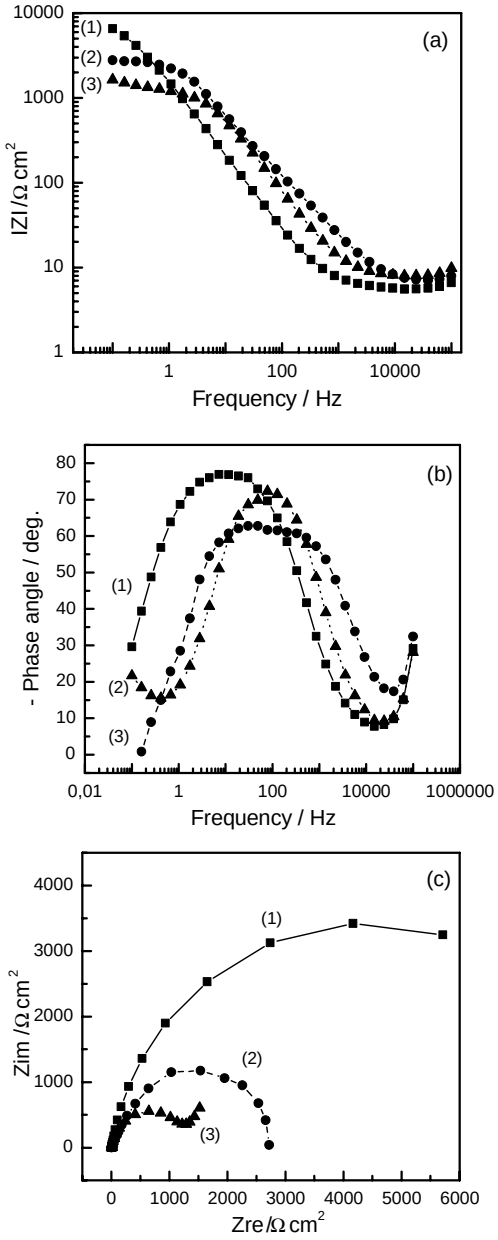

Fig. 9. Bode (a and b) and Nyquist (c) plots for the tested electrodes in 0.6 M NaCl solutions. Curves (1) for Al, (2) for Al–Ga–In and (3) for Al–In electrodes.

Bode (Figures 9a and 9b) and Nyquist (Figure 9(c)) plots for the tested electrodes in 0.6 M NaCl. As shown in Figure 9(a), at the high frequency limit, the impedance Z is dominated by the solution resistance R_s while at the very low frequency limit, the impedance approaches the sum of the solution resistance R_s and the polarization resistance R_p which is approximately equal to R_p. The slopes of the linear part in the log $|Z|$ against log f curves are equal to −0.83, −0.8, −0.69, for Al, Al–In and Al–Ga–In alloys, respectively, and not equal to −1. Furthermore, the phase shift at medium frequencies approaches values of about −78°, 72° and 62° for Al, Al–In and Al–Ga–In alloys, respectively, Figure 9(b). This may indicate that the capacitive behaviour (i.e., insulating behaviour) of the tested electrodes is affected as a result of alloying additions, where the oxide film formed on the Al surface exhibits good insulating properties and corrosion resistance compared with Al–In and Al–Ga–In alloys.

The Nyquist plots of Figure 9(c) show an incomplete capacitive semicircle for Al with a diameter of 8.5 k Ω cm^2 which represents the polarization resistance R_p. However, the capacitive semicircles obtained in the case of Al–In and Al–Ga–In alloys exhibit diameters of 1.35 and 2.85 k Ω cm^2, respectively. As seen in

Figure 9(c), the capacitive semicircle for Al–In electrode is followed by an almost linear region at low frequencies with an angle of about 45° with the real axis. This signifies a Warburg type impedance corresponding to a mass transfer process involving ionic diffusion. The tested electrodes can be arranged according to the increase in the polarization resistance, as determined from the capacitive loop, in the order:

$$\text{Al} > \text{Al–Ga–In} > \text{Al–In}$$

This indicates that Al–In alloy presents the most active behaviour compared with Al–Ga–In and pure Al electrodes which is in agreement with the aforementioned results.

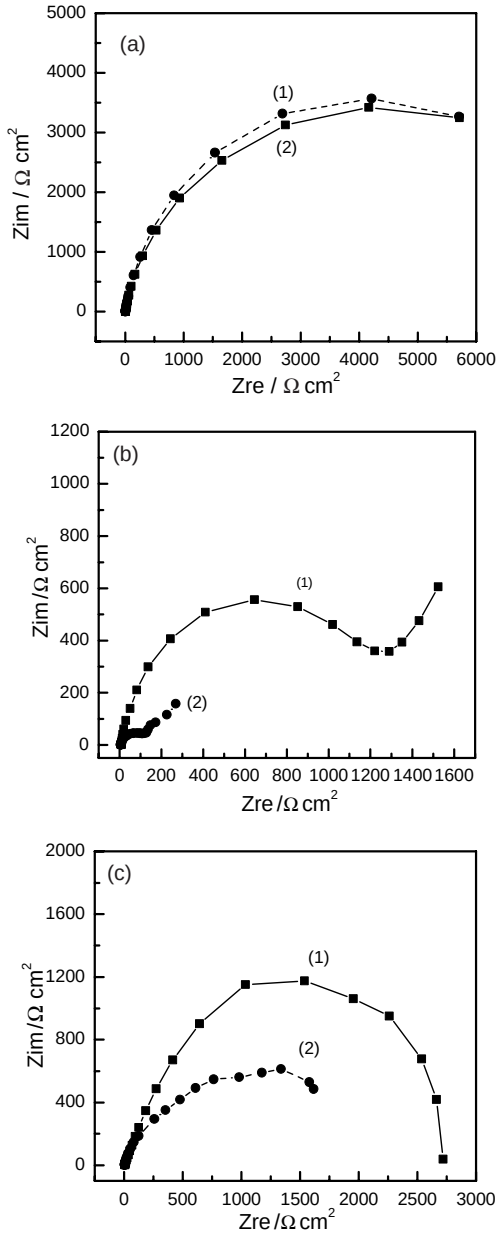

Fig. 10. Nyquist plots of (a) Al, (b) Al–In and (c) Al–Ga–In electrodes in 0.6 M NaCl without and with 0.01 M Zn^{2+}. Curves (1) without Zn^{2+} and (2) with 0.01 M Zn^{2+}.

Figure 10 presents Nyquist plots of Al, Al–In and Al–Ga–In electrodes in 0.6 M NaCl solutions containing 0.01 M Zn^{2+}. It is clearly seen that addition of Zn^{2+} has insignificant influence on the capacitive semicircle in the case of Al electrode, Figure 10(a), and hence on the polarization resistance, determined from the diameter of the semicircle. In contrast, addition of Zn^{2+} causes a large decrease in the polarization resistance in the case of Al–In alloy, 0.16 k Ω cm^2, Figure 10(b). Al–Ga–In alloy shows a moderate effect as a result of Zn^{2+} addition, since the polarization resistance takes a relatively lower value, 2.5 k Ω cm^2, in Zn^{2+} containing electrolyte compared with that obtained in Zn^{2+} free electrolyte, 2.85 k Ω cm^2, Figure 10(c). This signifies enhancement of the activity of Al–In and Al–Ga–In alloys in chloride solutions containing Zn^{2+} and supports the above results.

4. Conclusions

The outcome of the present work can be summarized as follows:

(i) Among the tested electrodes, Al–In alloy presents the highest negative open circuit potential in 0.6 M NaCl solution and the corrosion resistance of the tested electrodes decreases in the order: Al > Al–Ga–In > Al–In.

(ii) The initial dissolution of the Al–In electrode leads to increase the concentration of In^{3+} ions in the electrolyte, then the redeposition of In at active sites on the electrode surface occurs, leading to adsorption of Cl^- at high negative potential.

(iii) The potentiostatic I/t results in Zn^{2+} containing electrolytes at potentials more anodic than the pitting potential revealed that Zn^{2+} has insignificant influence on Al electrode, while it enhances the corrosion of Al–Ga–In alloy and improves the attack morphology of Al–In alloy.

(iv) Addition of Zn^{2+} to the electrolyte has insignificant influence on the polarization resistance of Al. However, in the case of Al–In and Al–Ga–In the polarization resistance showed a decrease in the presence of Zn^{2+}, signifying the activating effect of Zn^{2+} ions.

References

1. B.M. Ponchel and R.L. Horst, *Mater. Protect.* **7** (1968) 38.
2. M. Pourbaix, 'Atlas of Electrochemical Equilibria in Aqueous Solutions' (Pergamon, Oxford, 1966), p. 171.
3. D.S. Keir, M.J. Pryor and P.R. Sperry, *J. Electrochem. Soc.* **116** (1969) 319.
4. T. Valand and G. Nilsson, *Corros. Sci.* **17** (1977) 931.
5. D.R. Salinas and J.B. Bessone, *Corrosion* **47** (1991) 665.
6. M. Kliskić, J. Radosević and L.J. Aljinović, *J. Appl. Electrochem.* **24** (1994) 814.
7. S. Gudić, J. Radosević and M. Kliskić, *J. Appl. Electrochem.* **26** (1996) 1027.

8. S. Gudić, J. Radosević and M. Kliskić, *Impedance transient study of barrier films on aluminium and Al–Sn alloys*. Proceedings of the symposium on 'Passivity and its Breakdown', Electrochemical Society, New Jersey, (1997), p. 689.
9. A. Venugopal and V.S. Raja, *Corros. Sci.* **39** (1997) 2053.
10. A. Venugopal and V.S. Raja, *Br. Corros. J.* **31** (1996) 318.
11. S.B. Saidman, S.G. Garcia and J.B. Bessone, *J. Appl. Electrochem.* **25** (1995) 252.
12. C.B. Breslin, L.P. Friery and W.M. Carroll, *Corros. Sci.* **36** (1994) 85.
13. C.B. Breslin and W.M. Carroll, *Corros. Sci.* **34** (1993) 1099.
14. M.C. Reboul, PH. Gimenez and J.J. Rameau, *Corrosion* **40** (1984) 366.
15. A. Tamada and Y. Tamura, *Corros. Sci.* **34** (1993) 261.
16. C.D.S. Tuck, J.A. Hunter and G.M. Scamans, *J. Electrochem. Soc.* **134** (1987) 2070.
17. A.R. Despić, D.M. Drazić, M.M. Purenović and N. Ciković, *J. Appl. Electrochem.* **6** (1976) 527.
18. E. Aragon, L. Cazenave-Vergez, E. Lanza, A. Giround and A. Sebaoun, *Br. Corros. J.* **32** (1997) 121.
19. D. M. Drazić, S.K. Zecević and A.R. Despić, *Electrochim. Acta* **28** (1983) 751.
20. G. Burri, W. Luedi and O. Haas, *J. Electrochem. Soc.* **136** (1989) 2167.
21. J.E. Equey, S. Muller, J. Desilvestro and O. Haas, *J. Electrochem. Soc.* **139** (1992) 1499.
22. F. Holzer, S. Muller, J. Desilvestro and O. Haas, *J. Appl. Electrochem.* **33** (1993) 125.
23. W.M. Carroll and C.B. Breslin, *Br. Corros. J.* **26** (1991) 255.
24. C.B. Breslin, L.P. Friery and A. Rudd, *The role of indium and gallium in passivity breakdown of aluminium*. Proceedings of the symposium on 'Passivity and its Breakdown, Electrochemical Society', New Jersey (1997) p. 621.
25. S.B. Saidman and J.B. Bessone, *J. Appl. Electrochem.* **27** (1997) 731.
26. S.B. Saidman and J.B. Bessone, *Electrochim. Acta* **42** (1997) 413.
27. H.A. El Shayeb, F.M. Abd El Wahab and S. Zein El Abedin, *Corros. Sci.* **43** (2001) 655.
28. H.A. El Shayeb, F.M. Abd El Wahab and S. Zein El Abedin, *Corros. Sci.* **43** (2001) 643.
29. C.B. Breslin and W.M. Carroll, *Corros. Sci.* **33** (1992) 1735.
30. H.A. El Shayeb, F.M. Abd El Wahab and S. Zein El Abedin, *J. Appl. Electrochem.* **29** (1999) 601.
31. H.A. El Shayeb, F.M. Abd El Wahab and S. Zein El Abedin, *J. Appl. Electrochem.* **29** (1999) 473.
32. C.B. Breslin and L.P. Friery, *Corros. Sci.* **36** (1994) 231.
33. S. Zein El Abedin and A.O. Saleh, *J. Appl. Electrochem.* **34** (2004) 331.
34. F.A. Cotton and G. Wilkinson, Advanced Inorganic Chemistry, 4th edn (J. Wiley & Sons, New York, 1980), p. 334.
35. P.Li. Cabot, J.A. Garrido, E. Perez and J. Vingili, *Corros. Sci.* **26** (1986) 5.
36. C.B. Breslin, L.P. Friery and W.M. Carroll, *Corrosion* **49** (1993) 895.
37. A.G. Muñoz, S.B. Saidman and J.B. Bessone, *Corros. Sci.* **44** (2002) 2171.
38. A.M. Shams El-Din, F.M. Abd El Wahab and S.M. Abd El Haleem, *Werkst. Korros.* **5** (1973) 389.
39. R.G. Kelly, J.R. Scully, D.W. Shoesmith and R.G. Buchheit, in A. Philip and P.E. Schweitzer (Eds), 'Electrochemical Techniques in Corrosion Science and Engineering' (Marcel Dekker, New York, 2003), p. 83.